An SPC Monitoring System for Cycle-Based Waveform Signals Using Haar Transform

Shiyu Zhou, Baocheng Sun, and Jianjun Shi

***Abstract*—Due to the rapid development of computer and sensing technology, many measurements of process variables are readily available in manufacturing processes. These measurements carry a large amount of information about process conditions. It is highly desirable to develop a process monitoring and diagnosis methodology that can utilize this information. In this paper, a statistical process control monitoring system is developed for a class of commonly available process measurements—cycle-based waveform signals. This system integrates the statistical process control technology and the Haar wavelet transform. With it, one can not only detect a process change, but also identify the location and estimate the magnitude of the process mean shift within the signal. A case study involving a stamping process demonstrates the effectiveness of the proposed methodology on the monitoring of the profile-type data.**

***Note to Practitioners*—Cycle-based signal refers to an analog or digital signal that is obtained through automatic sensing during each operation cycle of a manufacturing process. The cycle-based signal is very common in various manufacturing processes (e.g., forming force in stamping processes, the holding force, and the current signals in spot welding processes, the insertion force in the engine assembly process). In general, cycle-based signals contain rich process information. In this paper, cycle-based signal monitoring will be accomplished by monitoring the wavelet transformation of the signal, instead of monitoring the raw observations themselves. Further, a decision-making technique is developed using the SPC monitoring system to locate where the mean shift occurred and to estimate magnitudes of mean shifts. Thus, this paper presents a generic framework for the enhanced statistical process control technique of cycle-based signals.**

***Index Terms*—Cycle-based waveform signals, Haar transformation, multivariate control charts, wavelet analysis.**

I. Introduction

DUE to the rapid development of sensing and computing technologies, many process variables are often measured in manufacturing processes. We consider the cycle-based waveform signals in discrete part manufacturing processes. As the name implies, a cycle-based waveform signal is an analog or digital signal that is obtained through automatic sensing during each operation cycle of a manufacturing process. Cycle-based waveform signals exist in many kinds of manufacturing processes (e.g., forming force in stamping processes, the holding force, and the current signals in spot welding processes, the insertion force in the engine assembly process). Fig. 1 illustrates the forming force (tonnage) signal in a stamping process.

These signals are measured during production cycles. The cycle-based waveform signals possess some interesting characteristics: 1) Within one cycle, the characteristics of the signal at different signal segments change significantly. For example, it is obvious that the frequency content of the segment between $90^\circ \sim 180^\circ$ is quite different from that of the segment $180^\circ \sim 270^\circ$ in the cycle-based signal shown in Fig. 1. The reason is that different segments of the cycle-based signal often correspond to different stages of the operation in one production cycle. 2) Between cycles, the signals are similar to each other but with some variation. This can be clearly seen from Fig. 1(b), the tonnages of these two cycles are aligned together according to the forming angle to illustrate the similarities and variation between these two cycles.

A cycle-based signal can be viewed as a high-dimensional multivariate random vector. In Fig. 1, each cycle-based signal contains 280 observation points. Therefore, the cycle-based signal can be viewed as a 280-dimensional random vector. Clearly, the components of the random vector are highly correlated. On the other hand, the variation between different signals is inevitable, which reflects the natural process variations due to the effects of inherent process disturbance factors, such as the randomness of lubrication distribution and material uniformity, etc. Under the same operational conditions, the disturbances of the process often do not change. Therefore, the signals of different cycles can be viewed as identically distributed samples of the random vector. Furthermore, the cycle-based signals are from discrete manufacturing processes. The time intervals between two production cycles are often much longer than the time constant of the process dynamics [1]. Therefore, the distribution of cycle-based signals can be assumed independent identically distributed (iid). The cycle-based signal contains a large amount of process-related information. Monitoring of cycle-based signals is a very interesting, yet challenging problem.

Some research has been done on the analysis and monitoring of waveform signals. The monitoring problem of linear profiles, which can be viewed as the simplest waveform signals, has been addressed in [2]–[5]. Jin and Shi [6] proposed an automatic diagnostic system for waveform signals. A training data set is required for the proposed method. Functional data analysis (FDA) [7] is a class of analysis methods that focuses on the analysis of "functional" data. FDA consists of data-analysis techniques

Manuscript received May 10, 2004; revised November 27, 2004. This paper was recommended for publication by Editor P. Ferreira upon evaluation of the reviewers' comments. This work was supported by the NSF Award DMII-0330356.

S. Zhou is with the Department of Industrial and Systems Engineering, University of Wisconsin, Madison, WI 53706 USA (e-mail: szhou@engr.wisc.edu).

B. Sun is with the Ford Motor Company, Dearborn, MI 48124 USA (e-mail: bsun@ford.com).

J. Shi is with the Department of Industrial Operations and Engineering, University of Michigan, Ann Arbor, MI 48105 USA (e-mail: shihang@umich.edu).

Digital Object Identifier 10.1109/TASE.2005.859655

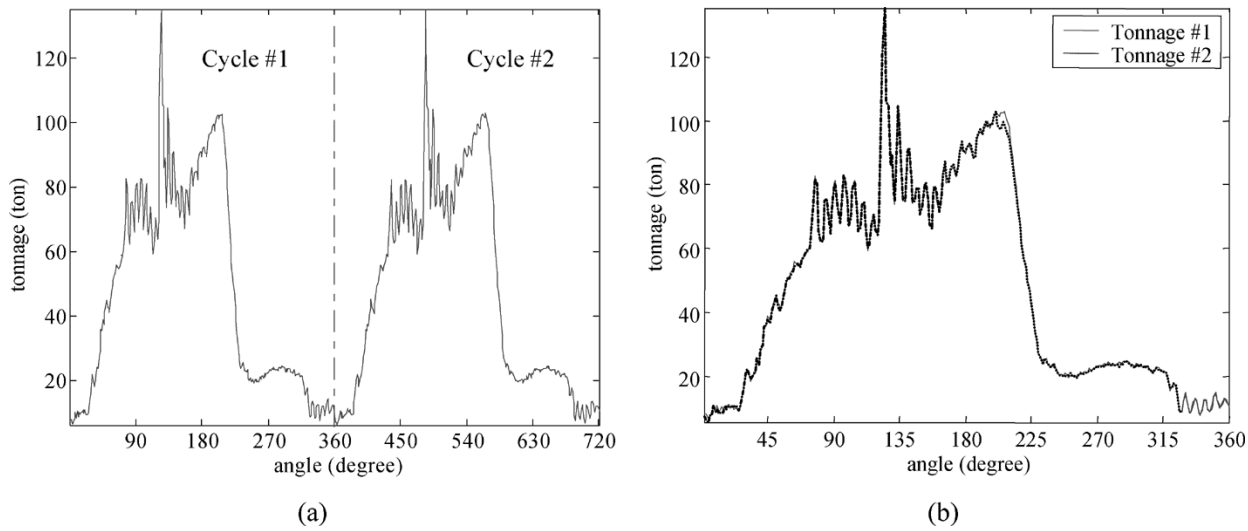

Fig. 1. (a) Forging tonnages of two cycles. (b) Overlapped tonnages of two cycles.

such as Fourier transformation, wavelet analysis, and functional principal component analysis, etc. Since a cycle-based waveform signal can be viewed as functional data, techniques from FDA can be applied to the cycle-based signal analysis. Actually, the method proposed in this article can be viewed as a special case in the FDA arena.

In this paper, the wavelet transforms will be used to represent the cycle-based waveform signals. The process monitoring will be accomplished by monitoring the wavelet coefficients, instead of monitoring the observations themselves. The wavelet transform is a very powerful tool in signal processing, which has been applied in various science and engineering fields with great success. In general, wavelet transforms are procedures that divide the data into both different time and frequency components. They have advantages over the traditional Fourier transform in analyzing signals with discontinuities and sharp spikes. Wavelet transformation particularly fits the needs of the analysis of cycle-based waveform signals. Comparing with other analytical bases, such as the Fourier bases, polynomial bases, etc., wavelet basis is designed to capture these localized features and the abrupt changes in the signals. Compared with the empirical bases, it is often easier to interpret the physical meanings of the wavelet coefficients. Based on the physical meaning, we can not only detect the changes in the signals, but also identify the location and possibly root causes of the changes. Hence, the monitoring of cycle-based waveform signal using wavelet transformation is preferable to other transformation methods.

Wavelet transformation has been used for process fault detection. The multiscale principal component analysis (MSPCA) method is proposed for the monitoring of continuous chemical processes [8], [9]. In MSPCA, PCA is conducted on the wavelet coefficients of each scale of a windowed sample of continuous processes. Then, the appropriate number of loadings of PCA and the wavelet coefficients are selected for each scale. Then, the selected coefficients are combined together, PCA is conducted again, and the signal is reconstructed. The final step is to monitor the process using the PCA of the reconstructed signal. There are a total of more than ten steps in the whole procedure [8]. Thus, the MSPCA is a somewhat complicated procedure. Furthermore, although PCA is very effective to detect the major variation directions in a data set, in some cases, it is difficult to interpret the physical meanings of the PCs. Most recently, Lada, *et al.* [10] developed a wavelet-based procedure for semiconductor process fault detection. They focused on the technique of selecting representing wavelet coefficients and a nonparametric procedure for detecting process faults based on the selected wavelet coefficients. Some researchers [11]–[13] have also used the Haar transform, one of the wavelet transforms, in fault detection and isolation by incorporating the engineering knowledge of the process. Wavelet analysis has also to be intensively used in the machine diagnosis based on process dynamic sensing signals. A group of researchers (Bukkapatnam, *et al.* [14]–[17], Suh, *et al.* [18], and Kamarthi, *et al.* [19]) have developed methodologies for chatter control, flank wear estimation, and machine fault diagnosis based on vibration, cutting force, and acoustic emission signals. In their work, wavelet analysis, chaos theory, and neural networks are combined together to parsimoniously represent the signal and efficiently extract the key features in the signal.

In this paper, a systematic statistical process control (SPC) monitoring system is proposed to integrate statistical process control with the Haar transformation in order to monitor cycle-based signals for the manufacturing processes. The rationale of using the Haar transform is discussed in Section II-A. The SPC system works as follows: 1) A set of cycle-based signals are collected. Each signal contains observations of a process variable during a production cycle. One cycle-based signal is viewed as one measurement sample. For the sake of convenience, we assume each signal has 2^p (p is a non-negative integer) data points. 2) A Haar transform is applied to each cycle-based signal, and Haar coefficients are calculated. 3) The total number of Haar coefficients is reduced by selecting the "significant" coefficients. 4) These remaining Haar coefficients are used as features of the process and they are monitored using a Hotelling T^2 statistic. 5) To interpret the T^2 chart, each Haar coefficient is monitored by an individual SPC chart with Bonforroni limits. 6) Based on the T^2 chart and individual charts of wavelet coefficients, an SPC monitoring "system" can be used to detect the mean-shift oc-

currence, to identify the location or time of the mean shift, and to estimate the mean-shift magnitude in the process.

The advantages of this SPC monitoring system are as follows: 1) By selecting the significant wavelet coefficients, the dimension of the sample vectors is dramatically reduced. Therefore, the performance of the SPC monitoring system for large dimensional data sets can be significantly improved. 2) By using a Haar transform and its inherent data structure, this SPC monitoring system facilitates the interpretation of T^2 statistic.

This paper is organized as follows. In next section, the Haar transform and its properties are briefly reviewed. Then, the SPC monitoring system is introduced. The application of the SPC monitoring system in the stamping tonnage signature monitoring is also given to illustrate the proposed SPC monitoring system. Finally, a summary is given in the last section.

II. SPC Monitoring System Using Haar Transform

A. Haar Transform and the Notation

The Haar transform is operated based on Haar functions, which consist of rectangular waves distinguished by time scaling and time shifts [20]. The set of continuous Haar functions $\{\varphi_n^m(x)\}$ is periodic, orthogonal, and complete. The sequence $\{\varphi_n^m(x)\}$ is defined in [0, 1] as

$$\varphi_0^0(x) = 1,\ x \in [0,1] \tag{1}$$

$$\varphi_n^m(x) = \begin{cases} 2^{\frac{(n-1)}{2}}, & \frac{(m-1)}{2^{n-1}} < x < \frac{\left(m-\frac{1}{2}\right)}{2^{n-1}} \\ -2^{\frac{(n-1)}{2}}, & \frac{\left(m-\frac{1}{2}\right)}{2^{n-1}} < x < \frac{m}{2^{n-1}} \\ 0, & \text{elsewhere}, \quad \forall x \in [0,1] \end{cases} \tag{2}$$

where n is the scale of the Haar transform and $1 \le m \le 2^{n-1}$ for $n \ge 1$. A function $f(x)$ can be approximated by a partial sum $S_N(x)$ containing 2^N terms, that is

$$S_N(x) = C_0^0 + \sum_{n=1}^{N} \sum_{m=1}^{2^{n-1}} \varphi_n^m(x) C_n^m \tag{3}$$

where C_n^m is called the mth Haar coefficient in scale n.

Discrete Haar functions are often used in practice. Define p as the smallest integer such that the number of observations does not exceed 2^p. Discrete Haar functions are obtained by sampling continuous Haar functions to produce a Haar array denoted by $\mathbf{H}_{N,p}$. Each row of $\mathbf{H}_{N,p}$ is a discrete Haar function obtained by sampling the continuous Haar function $\{\varphi_n^m(x)\}$ shown in (1) and (2). We let $h_{i,j}$ represent the i^{th} row of $\mathbf{H}_{N,p}$, which is generated as

$$h_{i,j} = 2^{-\frac{p}{2}} \varphi_n^m(j \cdot 2^{-p}), \quad 1 \le j \le 2^p \tag{4}$$

where $0 \le n \le N$, N is the scale number we selected, $1 \le m \le 2^{n-1}$, and $i = \begin{cases} 1, & \text{when } n = 0 \\ 2^{n-1} + m, & \text{when } n \ge 1 \end{cases}$. The multiplier $2^{-p/2}$ is used to normalize each row of $\mathbf{H}_{N,p}$. Usually, we have $p \ge N$. Each row of matrix $\mathbf{H}_{N,p}$ is orthogonal to each other.

If $\mathbf{x} = [x_1\ x_2\ \ldots\ x_{2^p}]^T$ is a sequence of 2^p discrete points, then the discrete Haar coefficients $\mathbf{c} = [c_0^0, c_1^1, c_2^1, c_2^2, c_3^1, \ldots, c_N^{2^N-1}]^T$ can be calculated as follows:

$$\mathbf{c} = \mathbf{H}_{N,p}\mathbf{x}. \tag{5}$$

The approximation of $\mathbf{x}$ using the Haar transform $\hat{\mathbf{x}}$ is given as follows:

$$\hat{\mathbf{x}} = \mathbf{H}_{N,p}^T \mathbf{c}. \tag{6}$$

The Haar coefficients have a relationship with mean values of the original signal over some intervals, as shown in (7) and (8).

For $n = 0$

$$C_0^0 = 2^{\frac{p}{2}} \bar{f}(1, 2^p). \tag{7}$$

For $n \ge 1$

$$C_n^m = 2^{\frac{(p-n-1)}{2}} \left[\bar{f}\left\{ (m-1)2^{(p-n+1)} + 1, \left(m - \frac{1}{2}\right) 2^{(p-n+1)} \right\} - \bar{f}\left\{ \left(m - \frac{1}{2}\right) 2^{(p-n+1)} + 1, m2^{(p-n+1)} \right\} \right] \tag{8}$$

where $\bar{f}(i,j) = (1/(j-i+1)) \sum_{k=i}^{j} x_k$. Thus, C_0^0 is proportional to the mean of $f(x)$. Every C_n^m except C_0^0, is proportional to the mean difference in two adjacent intervals.

From the above description, it can be seen that each coefficient of a Haar wavelet possesses clear interpretation: it is proportional to the mean difference of observations in two neighboring intervals, where the interval can be easily determined by the scale and translation. Because of this property, the mean shift of the signal among different segments can be easily calculated if the Haar coefficients are known. Therefore, the Haar transform fits very well with the control chart monitoring system. When the Haar transform is used to approximate observations within a cycle-based signal, possible mean shifts in the original signal can be captured by the Haar coefficients. Thus, Haar coefficients can be used as features to monitor the process for mean-shift detection and isolation.

B. Multivariate Control Chart Design

We use $\mathbf{x}_i$ to represent the ith cycle-based signal and $\{\mathbf{x}_i\}_{i=1}^{N_s}$ for a data set with N_s cycle-based signals. Each sample of the cycle-based signal $\mathbf{x}_i = [x_{1,i}, x_{2,i}, \ldots, x_{2^p,i}]^T$ has 2^p observations (p is a non-negative integer). The observations could be correlated within each cycle-based signal $\mathbf{x}_i$, $i = 1 \ldots N_s$ and we assume the multivariate samples $\{\mathbf{x}_i\}_{i=1}^{N_s}$ are iid normally distributed. The rationale behind this assumption is that the process variable is affected by many random disturbances existing in the process. Hence, the process variable tends to be normal due to the central limit theorem. Given the scale of the Haar transform N, $\mathbf{H}_{N,p}$ can be obtained by using (4). Then, Haar coefficients $\mathbf{c}_i$ can be computed for each sample $\mathbf{x}_i$ by using (5). Clearly, the Haar coefficients follow a multivariate normal distribution because they are linear combinations of normally distributed random variables from (5). Since the dimension of $\mathbf{c}_i$ is often much smaller than the dimension of $\mathbf{x}_i$, the T^2 statistic for the Haar coefficients instead of the signal itself is used to monitor the process. Thus, we use

$$T^2 = (\mathbf{c} - \bar{\mathbf{c}})^T \mathbf{S}^{-1} (\mathbf{c} - \bar{\mathbf{c}}). \tag{9}$$

To set up T^2 multivariate control charts on the individual observations, two phases are needed. The production is monitored in Phase II. The objective in Phase I is to obtain an in-control set of observations in order to establish the control limits in Phase II.

In Phase I, one significant issue is the robust estimation of covariance matrix of $\mathbf{c}$, which has been investigated in [21]. Here, we select the recommended method

$$\mathbf{S} = \frac{1}{2}\frac{\mathbf{V}^T\mathbf{V}}{N_s - 1} \tag{10}$$

where $\mathbf{V} = [(\mathbf{c}_2 - \mathbf{c}_1)^T \ (\mathbf{c}_3 - \mathbf{c}_2)^T \ \ldots \ (\mathbf{c}_{N_s} - \mathbf{c}_{N_s-1})^T]^T$. Due to this covariance estimation, the control limits for Phase I are

$$\begin{aligned} UCL &= \frac{(N_s-1)^2}{N_s}\beta_{\alpha,2^{N-1},\frac{(f-2^N-1)}{2}} \\ LCL &= 0, \end{aligned} \tag{11}$$

where $f = 2(N_s-1)^2/(3N_s-4)$, and $\beta_{\alpha,2^{N-1},(f-2^N-1)/2}$ is the upper α percentage point of a beta distribution with parameters 2^{N-1} and $(f-2^N-1)/2$.

In Phase II, the control limits are [21]

$$\begin{aligned} UCL &= \frac{2^N\left(N_s^2-1\right)}{N_s^2 - 2^N N_s}F_{\alpha,2^N,N_s-2^N} \\ LCL &= 0 \end{aligned} \tag{12}$$

where $F_{\alpha,2^N,N_s-2^N}$ is the upper α percentage point of an F distribution with parameters 2^N and $N_s - 2^N$. In Phase II, the covariance is estimated using the sample covariance matrix based on the in-control data points from Phase I

$$\mathbf{S} = \frac{1}{N_s - 1}\sum_{i=1}^{N_s}(\mathbf{c}_i - \overline{\mathbf{c}})(\mathbf{c}_i - \overline{\mathbf{c}})^T. \tag{13}$$

By specifying Type-I error probability α_1, the T^2 statistics based on Haar coefficients can be used to monitor the process. To implement this T^2 chart using the Haar transform, some practical issues need to be discussed.

C. Practical Issues in the Haar Transform

1) Scales to be Used in the Haar Transform: The problem of selecting scales is actually the problem of selecting the sufficient number of coefficients to represent the cycle-based signal. Based on the selected scale, a small number of wavelet coefficients are used to represent the original signal in the process monitoring step. This step is a very important step and several researchers have been working in this area. Jin and Shi [22] proposed a wavelet feature selection technique by integrating extensive engineering knowledge of the process. Bukkapatnam *et al.* [23] developed a wavelet packet representation of chaotic dynamic signals. Their method is for wavelet function design rather than wavelet coefficient selection. Lada *et al.* [10] and Pittner and Kamarthi [24] developed coefficient selection techniques based on the magnitude of the coefficients and a penalty on the number of coefficients.

In this paper, the selected coefficients are used for process monitoring using control charts techniques. To be successful, it is critical to not blur the difference between the in-control distribution and the out-of-control distribution in this step. If extensive information on both in-process (normal) distribution and out-of-control (abnormal) distribution is known, the coefficients can be selected to maximize the detection power under the same false alarm probability. However, in practice, the information, particularly the information of the out-of-control distribution, is quite difficult to obtain. In this paper, we propose a simple yet effective scale selection scheme based on limited information on the out-of-control distribution.

In this paper, we focus on the detection of the mean shifts or so-called "shape change" within the cycle-based waveform signal at certain intervals. Further, we assume that the interval of mean shift is large. These assumptions are determined by the requirement of specific processes (please refer to Section III). Based on this limited information regarding the out-of-control distribution, the coefficient selection is designed to select the coefficients of certain scales starting from the lowest scale of the wavelet transformation. Because the higher the scale used, the smaller the region of support for each Haar function in that scale; the very high scale coefficients can be ignored based on our information of the out-of-control distribution. This is the reason why we start from the lowest scale. Furthermore, the coefficients selected in this way can also simplify the interpretation of out-of-control points and the decision making procedure, which will be more clear in Sections II-D and II-E. The coefficient selection procedure is described as follows.

An index Q_i is defined to describe the satisfactory accuracy requirement by using the Haar transform for the sample of cycle-based signal $\mathbf{x}_i$, that is

$$Q_i = \frac{||\mathbf{x}_i - \hat{\mathbf{x}}_i||^2}{||\mathbf{x}_i||^2} \tag{14}$$

where $||\bullet||$ is the Euclidean norm of a vector and $\hat{\mathbf{x}}_i$ is the approximation of $\mathbf{x}_i$ using Haar transform with scale N.

It can be seen that the smaller the Q_i value, the better the fitting performance using the Haar transform for $\mathbf{x}_i$. If N_s samples are obtained for the process, given a satisfactory accuracy requirement Q, the Haar transform scale N used in a SPC monitoring system can be determined as follows:

$$N = \min(M|\max Q_i \le Q) \tag{15}$$

where Q_i is calculated by using (14) with Haar coefficient scale M for the ith sample $\mathbf{x}_i (1 \le i \le N_s)$. This means that the scale N is the minimum scale level such that for all of the samples, $Q_i \le Q$.

In the above scale level selection procedure, Q is often predetermined by the process and the signal characteristics. For example, if we know the mean shift happens within a interval of half the total length and the mean-shift magnitude is more than 10% of the signal magnitude, then the worst-case scenario of Q is to set Q as 5%. In the worst case, all of the signal change is captured by the high-scale wavelet coefficients that are ignored. However, this is the worst-case scenario because if the mean-shift interval is large, it is impossible that this mean shift will be only captured by high-scale coefficients. Therefore, the 5% value for Q will be sufficient. With other particular information regarding the out-of-control distribution, we can develop different schemes for wavelet coefficient selection.

To use this T^2 chart, we also need to check the effectiveness and adequacy of the coefficient selection in the statistical sense. Thus, similar to the Q statistic in principal component approach [25], the sum of squares of the residuals (SSR) in the coefficient selection should be checked. The SSR_i for the ith sample can be calculated as

$$\mathrm{SSR}_i = (\mathbf{x}_i - \hat{\mathbf{x}}_i)^{\mathrm{T}}(\mathbf{x}_i - \hat{\mathbf{x}}_i). \tag{16}$$

where SSR_i should be less than a prescribed threshold to ensure the effectiveness of the coefficient selection. Because the analytical distribution of SSR is very difficult to obtain, a nonparametric estimation method is used to estimate the distribution of SSR based on data. The threshold can be obtained based on the estimated distribution of SSR.

2) Signal Length Other Than a Power of Two: The discrete wavelet transformation is defined for sequences with a length of a power of two. Special measures need to be taken for other signal lengths. In practice, one straightforward treatment is to manipulate the original signal length by deleting certain signal segments that do not contain useful information. The selection of these signal segments should be based on the engineering knowledge of the operation stages of each cycle. For example, the forming force signal of stamping or forging processes often includes the sensor signals before the die hits the workpiece. Clearly, very little information is available in such a signal segment. Therefore, it is safe to delete that segment from the original signal to make the final length of the signal some power of two. If no signal segment can be safely deleted and the signal length is very close to some power of two, we can interpolate the original signal to change its length. The assumption of this method is that the signal is smooth and the interpolation will cause limited distortion of features of the signal, particularly, the features of interest.

Some researchers have proposed several methods for extending the signal length [26]: 1) zero-padding, in which zeros are added at the end of the signal; 2) symmetrization, in which the symmetric replications of the original signal around the end of the signal are used to extend the signal; 3) smooth padding, in which the extrapolation of the signal is used; and 4) periodic-padding, in which the periodic extension is used outside the original support of the signal. Although zero padding is the simplest extension method, it creates artificial discontinuities at the end of the signal. However, this discontinuity will only show up at very high scales. For the mean-shift detection purpose, the impact of zero-padding is limited. Therefore, zero-padding can still be considered in our case. The detailed discussion of extending the signal and corresponding impacts in wavelet transformation is out of the scope of this article. Interested readers can refer to [26] for more details.

3) Signal Alignment: A problem with the ordinary discrete wavelet transformation is its time-variant property (i.e., the coefficients of a delayed signal are not a time-shifted version of those of the original signal). This property is particularly troubling in the process monitoring and diagnosis application. The errors in the signal alignment will cause differences in the wavelet coefficients because of this time-variant property. Therefore, signal alignment is critical for the application of wavelet analysis.

Fortunately, signal alignment is not an issue for many cycle-based waveform signals because many of them can be naturally aligned. For example, the tonnage in stamping and forging are often sampled according to the crank angle of the press. They are crank angle indexed. We can just align the signal using the crank angle. In the engine head assembly process, the assembly force is sampled according to the relative distance of two mating parts. Thus, the signal alignment is also trivial for those cases. For the time-indexed cycle-based signal, a repeatable trigger can be used to identify the repeatable starting point of the signal. If such a trigger is not available, a data-driven method should be used. In FDA, signal alignment is called "functional data registration." The Newton–Raphson algorithm is used for the estimation of alignment. Registration can also be done using signification features or landmarks.

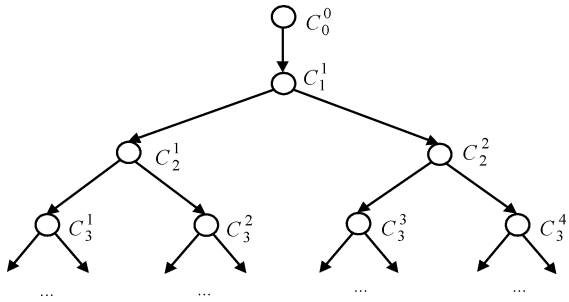

Fig. 2. Hierarchical structure of the SPC monitoring system.

D. Interpretation of Out-of-Control Signals

One challenge of the operation of the T^2 chart is the interpretation of the out-of-control point. Some work has been done on the interpretability of T^2 statistics. Murphy [27] proposed a procedure to identify the subset of variables, which account for a substantial portion of the observed value of the T^2 statistic. This procedure involves repeated calculation of the T^2 statistic by successively deleting various subsets of the variables from the computations. However, the performance of this approach regarding identification of the out-of-control variables becomes worse when the variables are correlated. With the T^2 decomposition approach [28], [29], one decomposes the T^2 statistic into individual components. Each decomposed component provides information about the variables that significantly contribute to an out-of-control signal.

Univariate control chart techniques can also be used to interpret the out-of-control points in the T^2 chart of Haar coefficients. The Haar coefficient $\mathbf{c}_i$ is a linear transformation of $\mathbf{x}_i$ by (5). Since $\mathbf{x}_i$ and $\mathbf{x}_j$, $i \neq j$, are assumed to be iid normally distributed, $\mathbf{c}_i$, $\mathbf{c}_j$, and $i \neq j$ are also iid normally distributed. Thus, Shewhart-type charts can be used to monitor each individual coefficient. There will be 2^N control charts, each of them monitors the mean shift at different intervals of the cycle-based signal. These 2^N control charts can be organized together in a hierarchical structure to form an SPC monitoring system, which is shown in Fig. 2. In manufacturing applications, a few charts of low-scale Haar coefficients will be sufficient for process monitoring.

Bonferroni's inequality approach is used by Alt [30] to interpret the out-of-control signal based on the individual control charts. In consideration of all the existing methods, Bonferroni's approach is chosen for out-of-control interpretation in our paper because it is very effective in detecting large mean shifts. On the other hand, when the dimension of variables is dramatically reduced using a Haar transform in the SPC monitoring system, Bonferroni control limits for each variable will become narrower than that based on the original signal. Thus, the dimension reduction based on the Haar transform

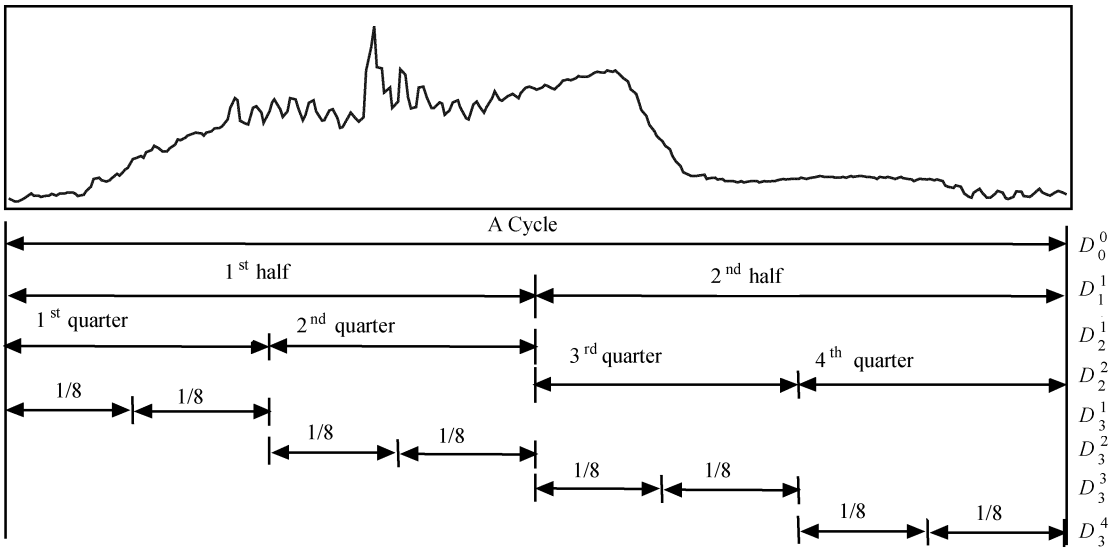

Fig. 3. Illustration of interval D_n^i.

in this SPC monitoring system also facilitates the Bonferroni approach.

When Hotelling T^2 chart in the SPC monitoring system indicates an out-of-control condition, each C_n^i will be checked for in control or out of control. Bonferroni's control limits are used for each C_n^i control chart, which are shown as follows:

$$\begin{aligned} CL_{C_n^i} &= \hat{u}_{C_n^i} \\ UCL_{c_n^i} &= \hat{u}_{c_n^i} + Z_{1-\frac{\alpha_1}{2p}} \hat{\sigma}_{C_n^i} \\ LCL_{C_n^i} &= \hat{u}_{C_n^i} - Z_{\frac{\alpha_1}{2p}} \hat{\sigma}_{C_n^i} \end{aligned} \tag{17}$$

where $CL_{C_n^i}$ is the central line, $UCL_{C_n^i}$ is the upper control limit, and $LCL_{C_n^i}$ is the lower control limit. The value α_1 is a preselected overall Type I error probability. We have $p = 2^N$. Also, $\hat{u}_{C_n^i}$ and $\hat{\sigma}_{C_n^i}$ are the estimated mean and standard deviation of C_n^i, respectively. Since each Haar coefficient is a linear combination of a set of segments of the original signal, its statistical properties are determined by the original signal and its region of support. The mean vector is estimated by

$$\hat{E}(\mathbf{c}) = \frac{1}{N_s} \sum_{i=1}^{N_s} \mathbf{c}_i \tag{18}$$

and the covariance matrix of $\mathbf{c}$ is estimated using (13).

It should be pointed out that Bonferroni's control limits for each Haar coefficient are used only for the interpretation of out-of-control T^2 statistics. The monitoring system Type I error probability has already been specified to be α_1 in the Hotelling T^2 chart for the Haar coefficients. There is a possibility that when the T^2 statistic indicates an out-of-control condition, all of the Haar coefficient control charts, however, indicate in-control. In this case, the individual control charts fail to interpret the out-of-control signals.

It can be seen from (7) that C_0^0 is proportional to the mean value of each cycle-based signal. Thus, the C_0^0 chart is equivalent to the conventional Shewhart-type chart for the mean. It has been shown in (8) that every C_n^i, except C_0^0, is proportional to the mean difference of observations in two adjacent intervals within a cycle. Thus, C_n^i charts, except the C_0^0 chart, monitor how the process mean changes at two subintervals within a cycle-based signal. As a result, the control charts for individual wavelet coefficients are inherently related in terms of their corresponding intervals. These interrelationships provide important information that can be used to determine mean-shift locations and their magnitudes. As a result, this SPC monitoring system can provide additional information that is not available in the conventional $\overline{X}$ chart and the Hotelling T^2 chart. When some mean shifts occur in certain positions of the cycle, the corresponding C_n^i charts will respond. By checking and analyzing the out-of-control charts, possible locations of mean shifts can be found. In this way, the proposed SPC monitoring system is used for not only process monitoring but also for the detection of the location of process change.

E. Decision-Making Methodology of SPC Monitoring System

If the T^2 chart for the Haar coefficients shows an out-of-control condition and the SSR chart shows an in-control condition, the SPC monitoring system is used to check which Haar coefficients are statistically out of control. Because of the special interrelationships among the Haar coefficients, in this section, we develop the decision-making methodology for the proposed SPC monitoring system to identify the locations (or occurrence times) of mean shifts in the cycle-based signal. In order to develop the decision-making methodology, some notation is defined as follows.

Definition 1: For a given sample, I_n^i is a Boolean indicator for a control chart C_n^i such that

$$I_n^i \equiv \begin{cases} 1 \text{ (true)}, & \text{if } C_n^i \text{ chart indicates in-control} \\ 0 \text{ (false)}, & \text{if } C_n^i \text{ chart indicates out-of-control.} \end{cases} \tag{19}$$

Definition 2: Interval D_n^i is defined as the region of support for the discrete Haar function $h_{2^{n-1}+i,j}$ $(j = 1, \ldots, 2^p)$. This support of the region corresponds to C_n^i.

The definition of interval D_n^i is illustrated in Fig. 3.

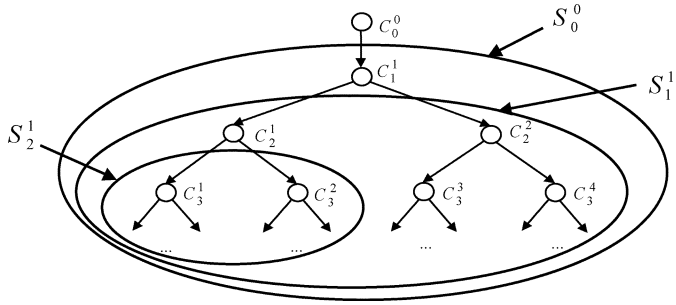

Fig. 4. Illustration of S_n^i.

Definition 3: S_n^i is a set of control charts of C_k^j, where k and j are non-negative integers and

$$\text{For } n = 0 \text{ and } i = 0,$$
$$S_0^0 = \left\{C_k^j\right\},\ 1 \le k \le N,\ 1 \le j \le 2^{k-1} \tag{20}$$
$$\text{For } n \ge 1 \text{ and } 1 \le i \le 2^{n-1},$$
$$S_n^i = \left\{C_k^j\right\},\ n+1 \le k \le N,$$
$$(i-1)\cdot 2^{k-n} + 1 \le j \le i \cdot 2^{k-n}. \tag{21}$$

An illustration of S_n^i is shown in Fig. 4.

Since the Haar coefficient C_n^i is very sensitive to the mean shift occurring in its support interval D_n^i $(n \ge 1)$, the mean-shift location could be identified by monitoring individual Haar coefficients. Thus, if there is an out-of-control alarm in an individual control chart of C_n^i, we can say that a mean shift occurred in C_n^i's supporting interval D_n^i. Since the supporting intervals of Haar coefficients at a higher scale are smaller than those of Haar coefficients at a lower scale, normally we can only report the mean shift corresponding to the higher scale coefficient if its interval overlaps with the interval of a lower scale coefficient that is also out of control. For example, if there are out-of-control alarms in the control charts of C_2^1 and C_1^1, since the corresponding support intervals $D_2^1 \subset D_1^1$, we only need to report that there is a possible mean shift in interval D_2^1. We can formulate this decision rule as follows. First, define an indicator function for the mean shift in the interval of D_n^i as DM_n^i, where $DM_n^i = 1$ if there is a mean shift in D_n^i and $DM_n^i = 0$, otherwise. Then

$$DM_n^i = \overline{I}_n^i \cap \left(\bigcap_{\forall C_k^l \in S_n^i} I_k^l \right) \tag{22}$$

where $\overline{I}_n^i$ is the logic NOT of I_n^i and $\cap$ is the logic AND operator. An interpretation of (22) is that there is a mean shift in D_n^i if the chart of C_n^i is out of control and other charts of C_k^j $(\forall C_k^j \in S_n^i)$ that are at higher scale levels and with overlapped supporting intervals are in control.

The first step in the decision-making procedure of SPC monitoring system is to check if the SSR chart for the Haar transform is in control or not. If it is not, the decision-making procedure should stop (The scales N used need to be increased to make the Haar transformation adequate.) The second step is to check the T^2 chart if the SSR chart is in control. If the T^2 chart is out of control, we would need to go to the third step to check the control charts for the individual Haar coefficients. Based on (22), the location of the mean shift can be further identified in the third step.

By using this decision-making procedure, we can not only detect the process change based on the T^2 chart, but also interpret the result of the T^2 chart based on the individual control charts of the Haar coefficients.

F. Mean-Shift Magnitude Estimation

Note that every interval D_n^i, except D_0^0, has two equal length subintervals by the definition of the Haar function. Thus, the magnitude of mean shifts can be estimated in the following two situations.

1) Estimation of the Mean-Shift Magnitude When $n = 0$: The magnitude of a mean shift in interval D_0^0 can be calculated as follows:

$$MS_0^0(1) = M_0^0(1) - \overline{M}_0^0(1) \tag{23}$$

where $MS_0^0(1)$ is the mean-shift magnitude of current sample in D_0^0. The value $M_0^0(1)$ is the estimated mean of the current sample in D_0^0, and $\overline{M}_0^0(1)$ is the mean value of the in-control data in D_0^0. It is clear that $M_0^0(1) = 2^{-p/2}\hat{C}_0^0$ and $\overline{M}_0^0(1) = 2^{-p/2}\overline{C}_0^0$, where $\overline{C}_0^0$ and $\overline{C}_0^0$ are the Haar coefficients at scale 0 of current cycle-based signal and the normal cycle-based signals, respectively.

2) Estimation of Mean-Shift Magnitude When $n \ge 1$: Since intervals D_n^i $(1 \le n \le N, 1 \le i \le 2^{n-1})$ consist of two equal-length subintervals, the estimation of the mean-shift magnitude should be done in two subintervals, shown as follows:

$$MS_n^i(k) = M_n^i(k) - \overline{M}_n^i(k) \tag{24}$$

where $MS_n^i(k)$ $(k = 1, 2)$ are the mean-shift magnitudes of the current sample in the first-half and the second-half interval of D_n^i. The values $M_n^i(k)$ and $\overline{M}_n^i(k)$ $(k = 1, 2)$ are the estimated mean values of the current cycle-based signal and the normal cycle-based signal in two subintervals of D_n^i, respectively.

In order to estimate the magnitude of mean shift for interval D_n^i, the magnitudes of mean values $M_n^i(k)$ $(k = 1, 2)$ should be calculated first. Using (8), the relationship between mean-shift magnitudes in two subintervals of D_n^i is

$$\left\{M_n^i(1) - M_n^i(2)\right\} = 2^{-\frac{(p-n-1)}{2}}\hat{C}_n^i. \tag{25}$$

Because $M_n^i(1)$ and $M_n^i(2)$ are the mean values in the first- and second-half interval of D_n^i, the following relation also exists with the mean value $M_{n-1}^j(k)$ of the interval D_{n-1}^j:

$$\frac{\left\{M_n^i(1) + M_n^i(2)\right\}}{2} = M_{n-1}^j(k) \tag{26}$$

where $1 \le n \le N$, $1 \le i \le 2^{n-1}$, and j and k are determined by n and i. Based on the fact that the interval covered by $M_{n-1}^j(k)$ is the interval covered by $M_n^i(1)$ and $M_n^i(2)$, the following rules can be obtained: if $n = 1$, then $j = 0$ and $k = 1$; if $n \ge 2$ and i is given, then j and k can be determined by $i = 2(j-1) + k$ where $k = 1, 2$ and $1 \le j \le 2^{n-2}$. For example, if $n = 3$, $i = 1$, then $j = 1$ and $k = 1$.

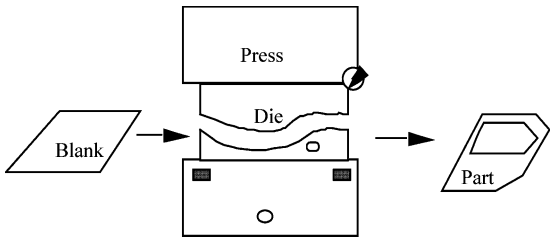

Fig. 5. Stamping process.

Since the calculation of mean values in scale n is based on the mean values in scale $n-1$, a recursive calculation is required to solve (25) and (26) together. The resulting solutions are

$$\begin{cases} M_n^i(1) = 2^{-\frac{(p-n+1)}{2}} \hat{C}_n^i + M_{n-1}^j(k) \\ M_n^i(2) = M_{n-1}^j(k) - 2^{-\frac{(p-n+1)}{2}} \hat{C}_n^i \end{cases} \text{ with initial value } M_0^0(1). \tag{27}$$

By using the same procedure of calculating $M_n^i(k)$ ($k = 1$, 2), $\overline{M}_n^i(k)$ ($k = 1$, 2) can be calculated using (27) and $\overline{C}_n^i$ in the place of $\hat{C}_n^i$. Finally, the mean-shift magnitudes $MS_n^i(k)$ ($k = 1$,2) can be estimated for the interval D_n^i by using (24).

III. Application of the SPC Monitoring System in Stamping Processes

A. Background

Stamping processes, as illustrated in Fig. 5, are important manufacturing processes. The current practice of stamping process control is based on offline manually inspecting part quality at specified time intervals. Therefore, there is a delay in fault detection. In a high-production rate environment, a large amount of scrap can be produced due to this delay. Hence, the offline manual inspection is not effective in preventing quality cost increase. It is highly desirable to develop an automatic process monitoring system for high-production rate stamping processes.

Little research has been reported in the process monitoring and fault diagnosis for stamping. Tonnage measurement contains rich information and features for stamping process failures [22]. One of very important forces to the part quality is the cushion force applied at a station. Cushion force is generated by the die cushion. Insufficient cushion forces resulting from air leakage will affect the part quality severely. The changes in cushion forces can be reflected in the tonnage signal mean shift within a certain stamping crank angle range.

The SPC monitoring system using Haar transforms developed in previous sections can be applied to monitor and diagnose the faults in cushion forces.

B. Stamping Process Monitoring by Using the SPC Monitoring System

In the stamping process considered in this case study, the cushion forming force (tonnage) of each production cycle is sampled (The data set is available upon request from the first author.) The sampling is with respect to the crank angle and each sample of the cycle-based signal consists of 280 measurement points. If we treat each measurement point as a variable, there are 280 process variables to describe the tonnage. There

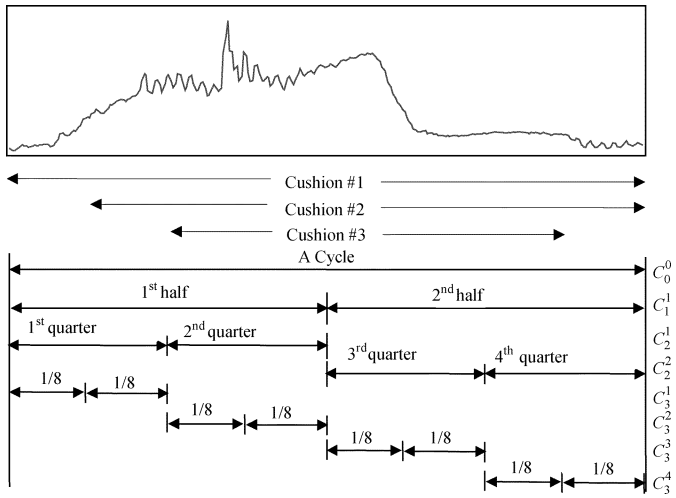

Fig. 6. Support regions for each control chart.

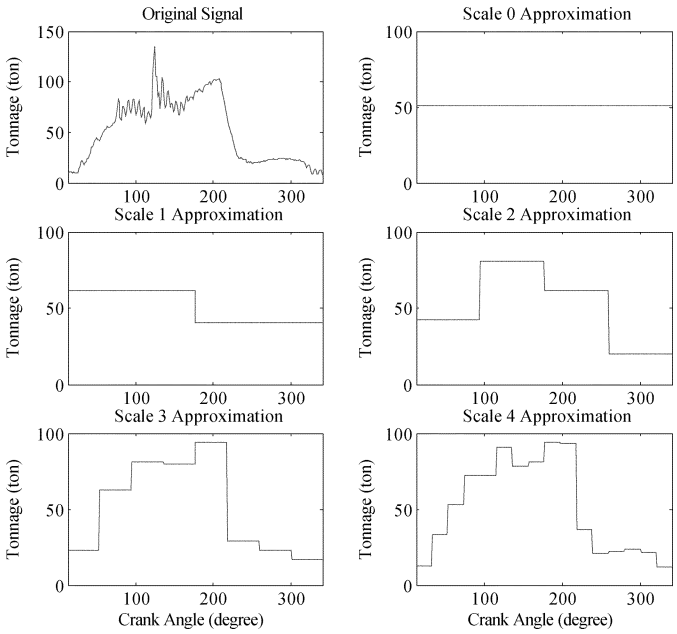

Fig. 7. Approximations of the original signal at different levels.

are three die cushions: cushion #1, cushion #2, and cushion #3. The cushion forces of cushion #1, #2, and #3 are associated with different crank angle ranges. For example, cushion #1 is related with all crank angles. If cushion #1 provides insufficient cushion force, a defective part is manufactured due to insufficient tonnage forces.

A total of 136 cycle-based signals are collected from this stamping process ($N_s = 136$) under normal conditions. Since the number of variables (280) is larger than the number of samples (136), the conventional T^2 chart could not be used here.

The Haar transform requires the number of observations to be some power of 2. In this study, 24 points are removed from the end of the original signal to create a new sample with 256 measurement points ($p = 8$). The support region for each Haar coefficient of the tonnage signal of one cycle is shown in Fig. 6. The approximations of the original signal using the first four levels of Haar coefficients are illustrated in Fig. 7.

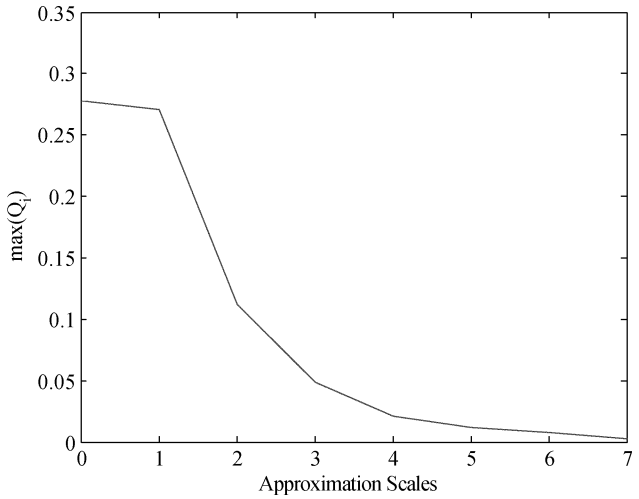

Fig. 8. Max Q_i with different Haar transform scales.

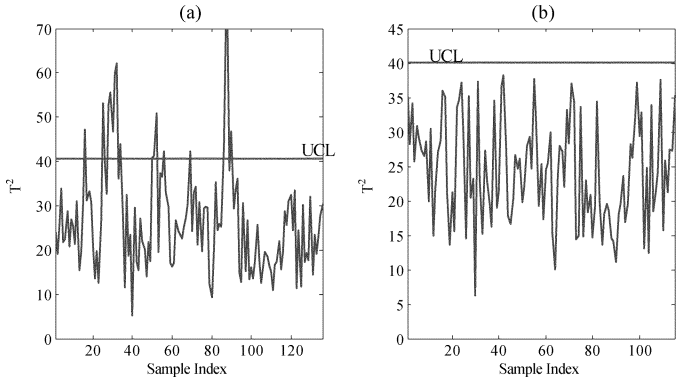

Fig. 9. Phase I T^2 chart.

The SPC monitoring system is built to monitor this stamping tonnage signal. By specifying $Q = 0.05$, the scale of the Haar transform is determined to be $N = 4$ by using (15). Max Q_i values with different Haar transform scales are shown in Fig. 8.

Each of the 136 cycle-based signals is used to perform the Haar transform, as in (5). The mean $\overline{\mathbf{c}}$ and sample covariance $\mathbf{S}$ of Haar coefficients can be calculated using (18) and (10), respectively. The Phase I T^2 chart with $\alpha_1 = 0.025$ is shown in Fig. 9. Fig. 9(a) is the Phase I T^2 chart for the original 136 cycle-based signals. Clearly, there are 21 out-of-control points. After those out-of-control points are removed, a new Phase I T^2 chart is implemented, as illustrated in Fig. 9(b). All of the 115 cycle-based signals are in-control in Fig. 9(b). Hence, these 115 cycle-based signals are taken as base-line in-control signals from normal working conditions. A typical normal signal is shown in Fig. 11.

With a lognormal distribution approximation of SSR, the SSR chart of the in-control cycle-based signals with $\alpha_2 = 0.0027$ is shown in Fig. 10. That the SSR chart is in control indicates the scales used by the Haar transform are appropriate.

In order to demonstrate the effectiveness of the SPC monitoring system developed in this paper, four cycle-based signals are collected at each of the three conditions: cushion #1 fault, cushion #2 fault, and cushion #3 fault. The fault in cushion #1

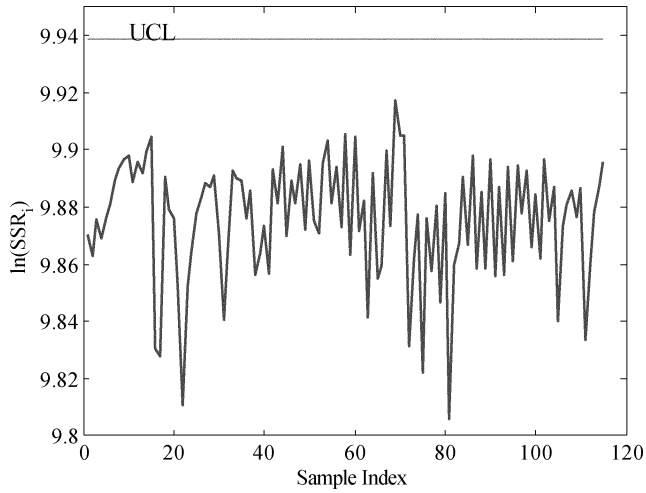

Fig. 10. SSR chart for the in-control signals.

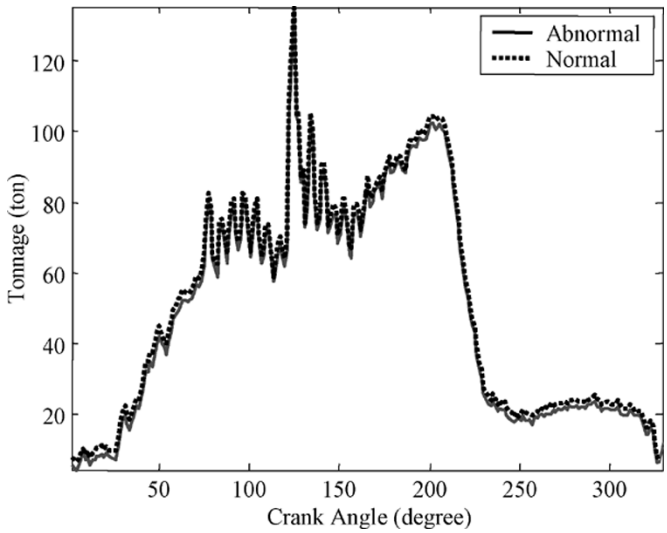

Fig. 11. Normal and abnormal signals.

happens in the first four samples. It causes a global mean shift within one operation cycle. The fault in cushion #2 happens in the next four samples. It causes a local mean shift from observation 34 to observation 256. The fault in cushion #3 happens in the final four samples. It causes local mean shifts from observation 68 to observation 226. Cycle-based signals from both a normal and a faulty condition (Fault #1) are shown in Fig. 11 (Other faulty signals are similar to the one shown: the difference between the normal signal and the faulty signal is not obvious from the original signal). It is difficult to detect and identify the location of the mean shift from the time-domain signals.

The outputs of the SPC monitoring system for these new samples are shown in Figs. 12 and 13. The vertical dashed lines in these two figures separate the data points of normal conditions and the data points of faulty conditions. To clearly illustrate the results, the log coordinate is used for the T^2 chart. In Fig. 12, the T^2 chart generates an out-of-control alarm for all of the data points from the faulty working condition. On the other hand, the SSR chart is in control. Therefore, by monitoring only 16 wavelet coefficients, we can detect the mean-shift changes of the cycle-based signals in this case study.

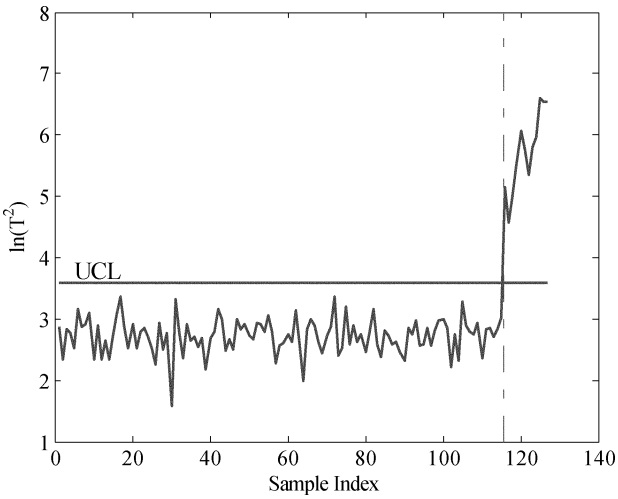

Fig. 12. T^2 chart.

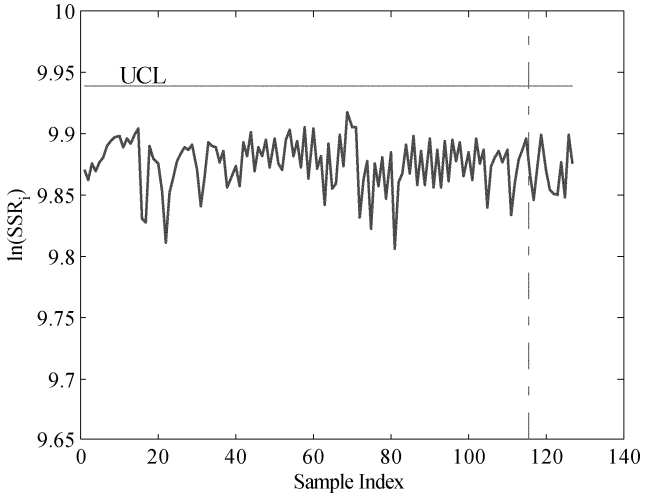

Fig. 13. SSR chart.

All individual charts C_n^i using Bonferroni limits are shown in Fig. 14 for these samples from the faulty working condition. The control limits are determined by (17), where α_1 is selected as 0.025.

The first sample is taken as an example to illustrate the decision-making method. According to Fig. 14, control chart C_0^0 is out of control in the first sample and other charts are in control. Thus, $I_0^0 = 0$ and other $I_n^i = 1$ by (19). By (22), $DM_0^0 = \bar{I}_0^0 \bigcap (\bigcap_{\forall C_k^l \in S_0^0} I_k^l) = \overline{0} \cap (\bigcap_{\forall C_k^l \in S_0^0} 1) = 1$. Thus, it can be concluded that a mean shift occurred in the interval D_0^0, which is consistent with the fact that a global mean shift occurred in the process signal. The results using this decision-making method are summarized in Table I. It can be seen from the figures and the table that the proposed SPC monitoring system can effectively detect the mean shift in the cycle-based signal.

For the fault caused by cushion #1, the estimated interval of mean shift is D_0^0, which is consistent with the fact that the fault in cushion #1 causes a global mean shift. For the fault caused by cushion #2, two of the samples indicate the mean shift occurred between 1∼64, one indicates that the mean shift happens between 1∼128, and one indicates that the mean shift is a global mean shift (1∼256). It should be pointed out that the Haar coefficients except C_0^0 represent the mean difference between the first half and the second half of their support intervals. Hence, the individual control charts of Haar coefficients are sensitive to the starting and ending location of the mean shifts, but not sensitive to the constant mean shift within their supporting intervals. Therefore, for a local mean shift as that caused by the fault of cushion #2, the SPC system can successfully identify the starting point of the mean shift (37th observation in this case) with high probability. The ending point of the mean shift for the fault caused by cushion #2 is the end of the cycle-based signal. Hence, there is no indication of the ending point before the end of the signal. Similarly, for the fault caused by cushion fault #3, the SPC system can successfully identify the starting and ending point for the mean shift (68th and 226th, respectively). Besides the location of the mean shift, the magnitude of the mean shift can also be estimated using (23) and (27). For example, for sample #1, the estimated mean shift is $MS_0^0(0) = -2.03$; for sample #5, the estimated mean shifts are $MS_3^1(1) = 0.1$ and $MS_3^1(2) = -2.6$.

It should be pointed out that all aforementioned system monitoring, mean-shift location detection, and mean-shift magnitude estimation can be automatically accomplished without operator intervention.

C. Statistical Performance Evaluation

The above application illustrates the effectiveness of the proposed SPC monitoring system. To evaluate the statistical performance, further numerical studies are conducted. In this study, the mean curve of the 115 base-line in-control cycle-based signals is taken as the true curve. In this simulation, the covariance structure is simplified. A normally distributed iid noise with zero mean and variance one was added to the mean curve to generate 100 cycle-based curves as the normal data set. Because the proposed method focuses on the mean-shift detection with fixed covariance, this simplification will not significantly affect the performance comparison. Then, three types of the control charts are implemented based on the normal data set: 1) a T^2 chart using 16 Haar coefficients. The α error probability is selected as 0.025 and the upper control limit is 37.44. 2) A χ^2 chart using the original 256-dimensional signal. The covariance matrix is the true value used in the simulation. (The T^2 chart is not used because of the difficulty of estimating the covariance of high dimensional data set.) The α error probability is selected as 0.025 and the upper control limit is 302.21. 3) A simple Shewhart chart that monitors the mean of the curve. The α error probability is also selected as 0.025. The center line is 51.11, the upper control limit is 51.26, and the lower control limit is 50.96.

To test the performance of these three control charts, 10 000 new cycle-based signals with different magnitudes of mean shift are generated and plotted on these three charts. The detection power $(1 - \beta)$ is estimated as the number of the out-of-control points divided by the 10 000. Four segments of mean shifts are considered: 1) the mean shift occurred on all 256 dimensions. 2) the mean shift occurred on 256/2 dimensions from observation #34 to #162. 3) the mean shift occurred on 256/4 dimensions from #162 to #226, and 4) the mean shift occurred on 256/4 dimensions from #33 to #65. The detection power of these three

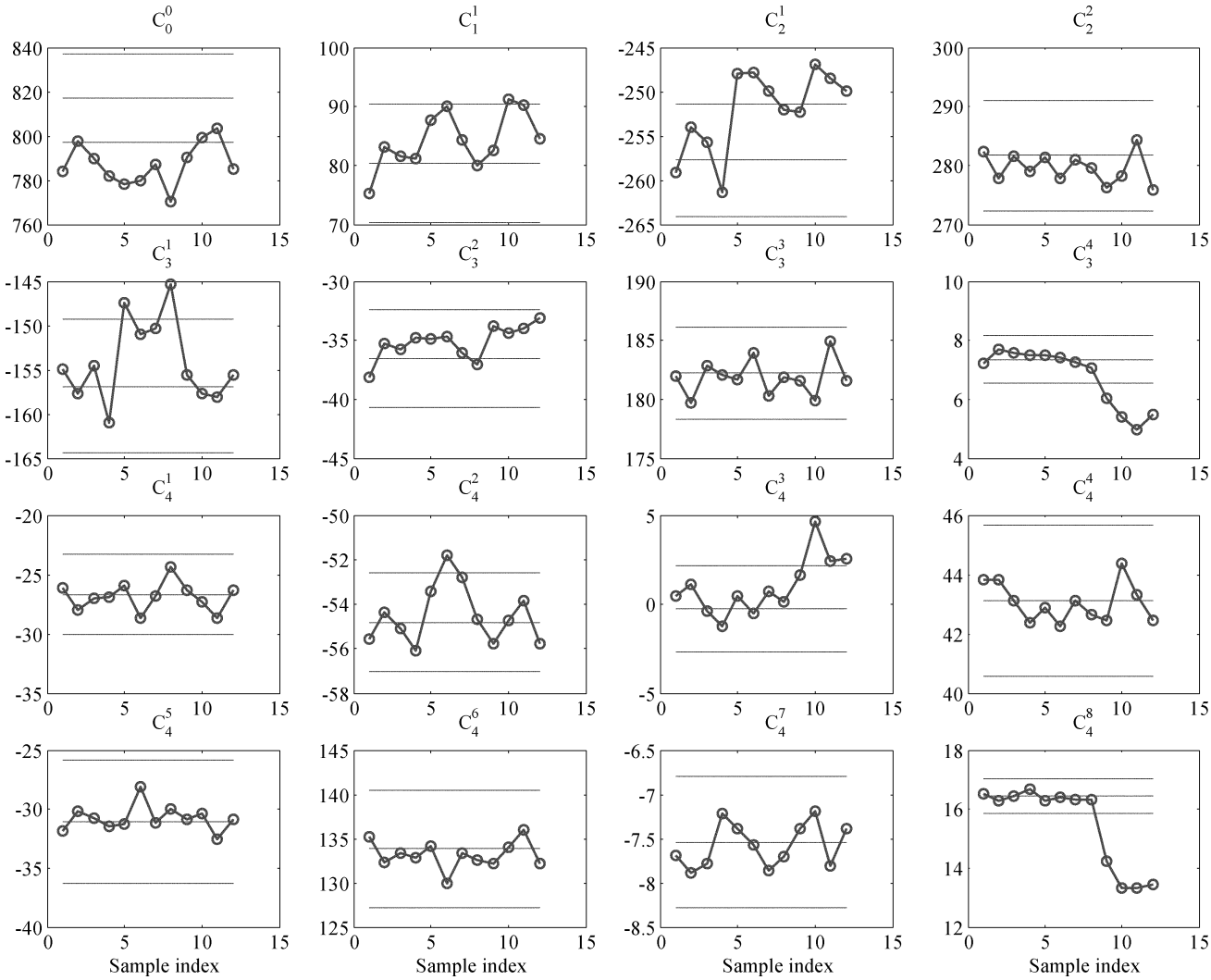

Fig. 14. C_n^i charts in the SPC monitoring system.

TABLE I
DECISION-MAKING RESULTS

Samples	Cushion Fault	I_n^i Support interval of the out-of-control coefficient	Intervals with mean shifts
1	#1	I_0^0	D_0^0(1~256)
2	#1	I_0^0	D_0^0(1~256)
3	#1	I_0^0	D_0^0(1~256)
4	#1	I_0^0	D_0^0(1~256)
5	#2	I_0^0, I_2^1, I_3^1	D_3^1(1~64)
6	#2	I_0^0, I_2^1, I_4^2	D_2^1 (32~64)
7	#2	I_0^0, I_2^1	D_2^1(1~128)
8	#2	I_0^0, I_3^1	D_3^1(1~64)
9	#3	I_0^0, I_3^4, I_4^8	D_4^8(225~256)
10	#3	$I_1^1, I_2^1, I_3^4, I_4^3, I_4^8$	D_4^3(65~96), D_4^8(225~256)
11	#3	$I_1^1, I_2^1, I_3^4, I_4^3, I_4^8$	D_4^3(65~96), D_4^8(225~256)
12	#3	$I_0^0, I_2^1, I_3^4, I_4^3, I_4^8$	D_4^3(65~96), D_4^8(225~256)

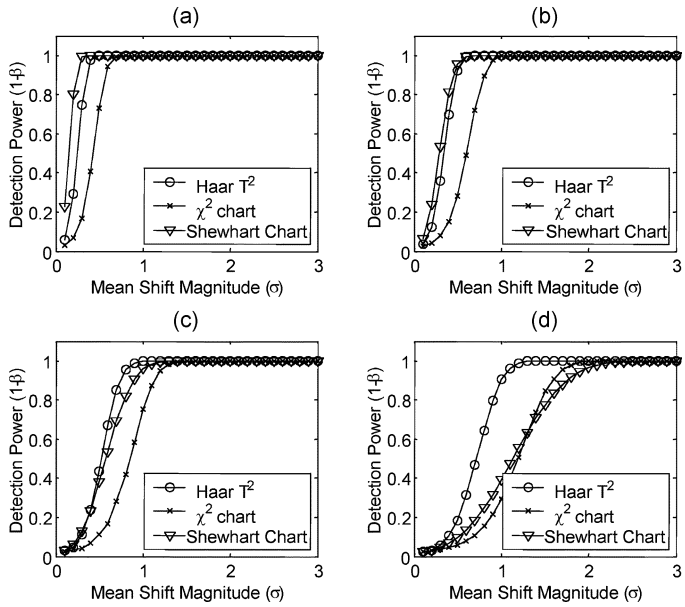

Fig. 15. Comparison of detection powers of the three types of control charts.

types of control charts for these cases of mean shift is shown in Fig. 15(a), (b), (c), and (d), respectively.

Based on Fig. 15, the detection power of the T^2 chart of the Haar coefficients is uniformly better than the detection power of the T^2 chart of the original signal. When the length of the mean-shift segment is long [Fig. 15(a) and (b)], the detection

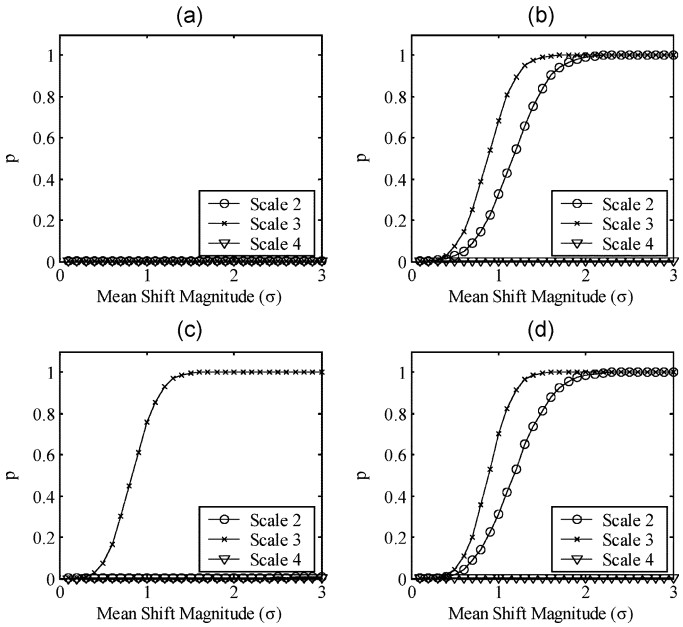

Fig. 16. Accuracy of the detection of the mean-shift location.

power of the Haar T^2 is comparable with the Shewhart chart. But when the mean-shift segment is short [Fig. 15(c) and (d)], the performance of Haar T^2 is much better than the Shewhart chart.

The accuracy of the detection of the mean-shift location is also studied. The results are shown in Fig. 16. The four subfigures correspond to the four cases of mean-shift segments as that in Fig. 15. In each subfigure, the probability of the detection of the starting point of the mean shift by the corresponding individual Bonferroni control charts, denoted as p, are illustrated. For example, consider Fig. 16(b). The mean shift occurred from observation #34 to #162. Since the support intervals of the wavelet coefficients C_2^1, C_3^1, and C_4^2 are #1∼#128, #1∼#64, and #33∼64, respectively, the wavelet coefficients that correspond to the starting point of the mean shift #34 at scale 2, 3, and 4 are C_2^1, C_3^1, and C_4^2, respectively. The three curves in Fig. 16(b) illustrate the detection probability of the individual Bonferroni control charts of these three coefficients. The overall α error of the Bonferroni charts is selected as 0.025.

From Fig. 16, we can see that in most cases, the proposed SPC monitoring system can successfully narrow down the location of the mean shift into a small interval. In Fig. 16(b), (c), (d), the coefficient at Scale 3 possess good detection power for all of the three mean-shift cases. Since the support interval of Scale 3 coefficient is with length of 64, we can narrow down the mean-shift location to an interval with a length of 64. Another significant characteristic that can be seen from Fig. 16 is that the detect power is affected by the location of the starting point of the mean shift. This is not surprising because the Haar coefficient is proportional to the mean difference of observations in two neighboring intervals. If the mean-shift segment covers the whole support of a Haar coefficient or the mean-shift segment is symmetric to the middle point of the support of a Haar coefficient, the corresponding Haar coefficient will be insensitive to the mean shift. For example, in Fig. 16(a), the mean-shift segment covers the whole cycle-based signal. Although the T^2 chart using Haar coefficients possesses high detection power in this case [Fig. 15(a)], the high scale individual coefficients are not sensitive to this mean shift. In Fig. 16(c), the mean-shift segment is from #162 to #226, which is almost symmetric to the middle point of C_2^2 (#192). Therefore, C_2^2 is not sensitive to this mean shift in Fig. 16(c). On the other hand, if the mean-shift segment is located in one subinterval of the support interval, the corresponding Haar coefficient will be most sensitive.

From these numerical studies, the proposed SPC monitoring system possesses good detection power and detection accuracy for the mean shift in cycle-based signals. One limitation of this method that can also be seen from the simulation is that accuracy of the detection of the mean-shift location is affected by the location of the mean-shift segment. This limitation is due to the inherit data structure of the Haar transform. A generalized Haar transformation that can overcome this limitation is currently under investigation. The results will be reported in the near future.

IV. Summary and Discussion

A new SPC monitoring system is developed in this paper by integrating statistical process monitoring and wavelet transform. This system provides the capability of automatically detecting the mean shifts in cycle-based process signals. It has many advantages over the conventional multivariate SPC charts.

First, this system provides a systematic statistical monitoring approach. It can be used to analyze the monitored process at different scales (frequencies) by using the hierarchical structure of the SPC monitoring system. Decision-making using the SPC monitoring system can be used to locate where the mean shift occurred and to estimate magnitudes of mean shifts. Second, when the number of observations within a sample is very large, the conventional T^2 chart is difficult to use due to the high dimensionality of the variable space. Similar to the principal component approach to reduce the dimensionality of data, the proposed SPC monitoring system utilizes the Haar transform as a dimension reduction tool. A Hotelling T^2 chart is used to monitor the Haar coefficients. Because the Haar coefficients are very sensitive to the systematic mean shift within each sample, the proposed SPC monitoring system is very effective in mean-shift detection. If other signal characteristics (e.g., the frequency content) are important, a different wavelet basis can be used. An example of sheet metal stamping tonnage signal monitoring is provided to demonstrate the effectiveness of the developed SPC monitoring system. It is shown that for processes with systematic mean shifts within a sample, the proposed SPC monitoring system provides more information and detection capability than conventional SPC methods.

This paper presents a generic framework for the enhanced statistical process control technique for cycle-based process signals. The case study illustrates the potential for the proposed methodology. In the future, several remaining issues in this scheme will be studied quantitatively, such as the impact of the scale selection on the performance of the control charts, and the relationship between the magnitude, location of the process mean shift, and the probability of detection.

ACKNOWLEDGMENT

The authors would like to thank the editors and reviewers for their insightful comments and suggestions, which have improved the paper quality and readability. We would also like to express our gratitude to Prof. Jin for providing stamping tonnage data for the case study.

REFERENCES

[1] D. C. Montgomery, *Introduction to Statistical Quality Control*, 4th ed. New York: Wiley, 2001.
[2] L. Kang and S. L. Albin, "On-line monitoring when process yields a linear profile," *J. Quality Technol.*, vol. 32, pp. 418–426, 2000.
[3] K. Kim, M. A. Mahmoud, and W. H. Woodall, "On the monitoring of linear profiles," *J. Quality Technol.*, vol. 35, no. 3, pp. 317–328, 2003.
[4] M. A. Mahmoud and W. H. Woodall, "Phase I Monitoring of Linear Profiles with Calibration Applications," *Technometrics*, vol. 46, no. 4, pp. 380–391, 2004.
[5] W. H. Woodall, D. J. Spitzner, D. C. Montgomery, and S. Gupta, "Using control charts to monitor process and product quality profiles," *J. Quality Technol.*, vol. 36, no. 3, pp. 309–320, 2004.
[6] J. Jin and J. Shi, "Automatic feature extraction of waveform signals for in-process diagnostic performance improvement," *J. Intell. Manuf.*, vol. 12, pp. 267–268, 2001.
[7] J. Ramsay and B. Silverman, *Functional Data Analysis*. New York: Springer-Verlag, 1997.
[8] B. R. Bakshi, "Multiscale PCA with application to multivariate statistical process monitoring," *AIChE J.*, vol. 44, no. 7, pp. 1596–1610, 1998.
[9] P. Teppola and P. Minkkinen, "Wavelets for scrutinizing multivariate exploratory models—interpreting models through multiresolution analysis," *J.Chemometrics*, vol. 15, pp. 1–18, 2001.
[10] E. K. Lada, J.-C. Lu, and J. R. Wilson, "A wavelet-based procedure for process fault detection," *IEEE Trans. Semicond. Manuf.*, vol. 15, no. 1, pp. 79–90, Feb. 2002.
[11] C. K. H. Koh, J. Shi, and W. J. Williams, "Tonnage signature analysis using the orthogonal (Haar) transforms," *NAMRI/SME Trans.*, pp. 229–234, 1995.
[12] C. K. H. Koh, J. Shi, and J. Black, "Tonnage signature attribute analysis for stamping process," *NAMRI/SME Trans.*, vol. 23, pp. 193–198, 1996.
[13] C. K. H. Koh, J. Shi, W. J. Williams, and J. Ni, "Multiple fault detection and isolation using the Haar transform, part I: theory," *ASME Trans., J. Manuf. Sci. Eng.*, vol. 121, pp. 290–294, 1998.
[14] S. Bukkapatnam, A. Lakhtakia, and S. Kumara, "Conceptualization of Chaos theory based optimal cutting tool chatter control," *Speculations Sci. Technol.*, vol. 19, pp. 137–148, 1996.
[15] ——, "Chaotic neurons for on-line quality control in manufacturing," *Int. J. Advanced Manuf. Technol.*, vol. 13, pp. 95–100, 1997.
[16] S. Bukkapatnam, S. Kumara, and A. Lakhtakia, "Analysis of acoustic emission signals in machining," *ASME Trans. Manuf. Sci. Eng.*, vol. 121, pp. 568–576, 1999.
[17] ——, "Fractal estimation of flank wear in turning," *J. Dynam. Syst., Measure., Contr.*, vol. 122, pp. 89–94, 2000.
[18] J. Suh, S. R. T. Kumara, S. Mysore, D. Lang, and A. Garga, "Wavelets assisted condition monitoring of heavy equipment," *Ann. Int. Inst. Prod. Eng. Res. (Annals of CIRP)*, 1999.
[19] S. V. Kamarthi, S. R. T. Kumara, and P. H. Cohen, "Flank wear estimation in turning through wavelet representation of acoustic emission signals," *Trans. ASME, J. Manuf. Sci. Eng.*, pp. 12–19, 2000.
[20] C. S. Burrus, R. A. Gopinath, and H. Guo, *Introduction to Wavelets and Wavelet Transforms: A Primer*. Upper Saddle River, NJ: Prentice-Hall, 1998.
[21] J. H. Sullivan and W. H. Woodall, "A comparison of multivariate control charts for individual observations," *J. Quality Technol.*, vol. 28, no. 4, pp. 398–408, 1996.
[22] J. Jin and J. Shi, "Feature-preserving data compression of stamping tonnage information using wavelets," *Technometrics*, vol. 41, pp. 327–339, 1999.
[23] S. Bukkapatnam, S. Kumara, and A. Lakhtakia, "Local Eigenfunction based suboptimal wavelet packet representation of contaminated chaotic signals," *IMA J. Appl. Math.*, pp. 1–23.
[24] S. Pittner and S. Kamarthi, "Feature extraction from wavelet coefficients for pattern recognition tasks," *IEEE Trans. Pattern Anal. Mach. Intell.*, vol. 21, no. 1, pp. 83–88, Jan. 1999.
[25] J. E. Jackson, "Control procedures for residuals associated with principal component analysis," *Technometrics*, vol. 14, pp. 341–349, 1979.
[26] G. Strang and T. Nguyen, *Wavelets and Filter Banks*. Wellesley, MA: Wellesley-Cambridge, 1996.
[27] B. J. Murphy, "Selecting out of control variables with the T^2 multivariate control procedure," *Statistic.*, vol. 36, pp. 571–583, 1987.
[28] R. L. Mason, N. D. Tracy, and J. C. Young, "Decomposition of T^2 for multivariate control chart interpretation," *J. Quality Technol.*, vol. 27, pp. 99–108, 1995.
[29] ——, "A practical approach for interpreting multivariate T^2 control chart signals," *J. Quality Technol.*, vol. 29, pp. 396–406, 1997.
[30] F. B. Alt, "Multivariate quality control," in *Encyclopedia of the Statistical Sciences*, N. L. Johnson, S. Kotz, and C. R. Read, Eds. New York: Wiley, 1984.

Shiyu Zhou received the B.S. and M.S. degrees in mechanical engineering from the University of Science and Technology of China, Hefei, in 1993 and 1996 respectively, and the M.Sc. degree in industrial engineering and Ph.D. degree in mechanical engineering from the University of Michigan, Ann Arbor, in 2000.

Currently, he is an Assistant Professor in the Department of Industrial Systems Engineering, University of Wisconsin-Madison. His research interests are the in-process quality and productivity improvement methodologies by integrating statistics, system and control theory, and engineering knowledge. The objective is to achieve automatic process monitoring, diagnosis, compensation, and their implementation in various manufacturing processes. His research is sponsored by National Science Foundation, Department of Energy, NIST-ATP, and industries.

Dr. Zhou is a member of the Institute of Industrial Engineers (IIE), Institute for Operating Research and the Management Sciences (INFORMS), American Society of Mechanical Engineers (ASME), and the Society of Manufacturing Engineers (SME).

Baocheng Sun received the B.S. degree in electrical engineering fromo Jilin Institute of Technology, Changchun, China, in 1987, the M.S. degree in electrical engineering at Beijing Institute of Technology, Beijing, China, in 1990, the Ph.D. degree in electrical engineering from the Institute of Automation, Chinese Academia of SINICA, Beijing, in 1994, and the Ph.D. degree in industrial operations and engineering at the University of Michigan, Ann Arbor, in 2000.

Currently, he is an Engineering Supervisor with V-Engine Engineering, Ford Motor Company, Dearborn, MI. His research interests are in-process quality and improvement methodologies, artificial neural networks, and reliability and robustness of automotive component/systems.

Jianjun Shi received the B.S. and M.S. degrees in electrical engineering from the Beijing Institute of Technology, Beijing, China, in 1984 and 1987, respectively, and the Ph.D. degree in mechanical engineering from the University of Michigan, Ann Arbor, in 1992.

Currently, he is a Professor in the Department of Industrial and Operations Engineering, University of Michigan, Ann Arbor. His research interests include the fusion of advanced statistical and domain knowledge to develop methodologies for modeling, monitoring, diagnosis, and control for complex manufacturing systems. His research has been funded by the National Science Foundation, NIST Advanced Technology Program, General Motors, Daimler-Chrysler, Ford, Lockheed-Martin, Honeywell, and various other industrial companies and funding agencies.

Dr. Shi is a member of American Society of Mechanical Engineers (ASME), American Society for Quality (ASQ), the Institute of Industrial Engineers (IIE), and the Society of Manufacturing Engineers (SME).